Anomalous enhancement of tetragonality in $PbTiO_3$ induced by negative pressure

Silvia Tinte, Karin M. Rabe and David Vanderbilt
Department of Physics and Astronomy, Rutgers University, Piscataway, New Jersey 08854-8019, USA
(Dated: June 7, 2003)

Using a first-principles approach based on density-functional theory, we find that a large tetragonal strain can be induced in $PbTiO_3$ by application of a *negative* hydrostatic pressure. The structural parameters and the dielectric and dynamical properties are found to change abruptly near a crossover pressure, displaying a "kinky" behavior suggestive of proximity to a phase transition. Analogous calculations for $BaTiO_3$ show that the same effect is also present there, but at much higher negative pressure. We investigate this unexpected behavior of $PbTiO_3$ and discuss an interpretation involving a phenomenological description in terms of a reduced set of relevant degrees of freedom.

PACS numbers: 61.50.Ks, 77.84.Dy, 81.05.Zx

I. INTRODUCTION

Recent work has shown that single-crystal solid-solution ferroelectric perovskites can have dramatically improved electromechanical properties compared to conventional transducer materials.[1,2,3] Representative materials include $PbZn_{1/3}Nb_{2/3}O_3$–$PbTiO_3$ and $PbMg_{1/3}Nb_{2/3}O_3$–$PbTiO_3$, which have ultrahigh piezoelectric coefficients and low dielectric loss. These materials have also been observed to exhibit electric-field induced phase transformations to "ultrahigh" strain states.[1]

$PbTiO_3$ serves as the common parent compound for this class of materials, and may be supposed to play an important role in the observed behavior. Since the discovery of ferroelectricity in perovskite oxides in the 1950's, $PbTiO_3$ has been the focus of extensive experimental and theoretical study. It has a single phase transition at $T_c = 766$ K from a paraelectric cubic phase to a ferroelectric tetragonal phase, and a c/a of 1.06 at low temperature. The structure and properties of $PbTiO_3$ have been widely studied using first-principles calculations.[4,5,6,7,8] Nevertheless, we report here a feature of the behavior of $PbTiO_3$ that had not previously been noticed. Our calculations show that an enormous tetragonal strain can be induced in $PbTiO_3$ by application of a *negative* hydrostatic pressure. The structural parameters, such as cell volume and atomic displacements, are found to change abruptly near a crossover pressure, displaying a "kinky" behavior suggestive of proximity to a phase transition. Analogous calculations for $BaTiO_3$ show that the same effect is also present there, but at much higher negative pressure.

In this paper, we investigate this unexpected behavior of $PbTiO_3$, and discuss its interpretation using a phenomenological description in terms of a reduced set of relevant degrees of freedom. We make the notion of proximity to a phase transition more precise by demonstrating that small changes in the parameters in this description can take the system through a triple point, leading to first-order transition behavior. Although the application of negative pressure is not feasible experimentally, our theoretical study provides useful insights into the structural instabilities of $PbTiO_3$, and may ultimately help suggest other, more practical avenues leading to enhanced tetragonality in $PbTiO_3$ and related compounds.

The paper is organized as follows. Section II provides the technical details of our first-principles calculations. Sec. III gives the results of our computations for the tetragonal distortion, structural parameters, and lattice dynamical properties as a function of applied negative pressure. In Sec. IV we introduce a phenomenological model that allows us to identify the relevant degrees of freedom responsible for this behavior, and we conclude with a brief discussion in Sec. V.

II. COMPUTATIONAL DETAILS

All *ab initio* calculations were performed in the framework of the Hohenberg-Kohn-Sham density-functional theory (DFT) within the local-density approximation (LDA). We use the ABINIT package,[9] a plane-wave pseudopotential code that, in addition to ground-state total-energy and force calculations, allows linear-response computations of phonon frequencies and Born effective charges. Our calculations use the Perdew-Wang[10] parameterization of the Ceperley-Alder[11] exchange-correlation, and the extended norm-conserving pseudopotentials of Teter.[12] These pseudopotentials include the O $2s$ and $2p$, the Ti $3s$, $3p$, $3d$ and $4s$, the Ba $5s$, $5p$ and $6s$, and the Pb $5d$, $6s$ and $6p$ in the valence states. We have used an energy cutoff of 60 Ha throughout. The integrals over the Brillouin zone have been replaced by a sum over a $6\times6\times6$ **k**-point mesh. Convergence of the relaxations requires the Hellmann-Feynman forces to be less than 0.003 eV/Å. We have computed the eigenvalues and eigenvectors of zone-center force-constant matrices by using both finite-difference (frozen-phonon) and linear-response approaches (with typical displacements of ±0.007 a.u. for the former), finding excellent agreement between the two schemes.

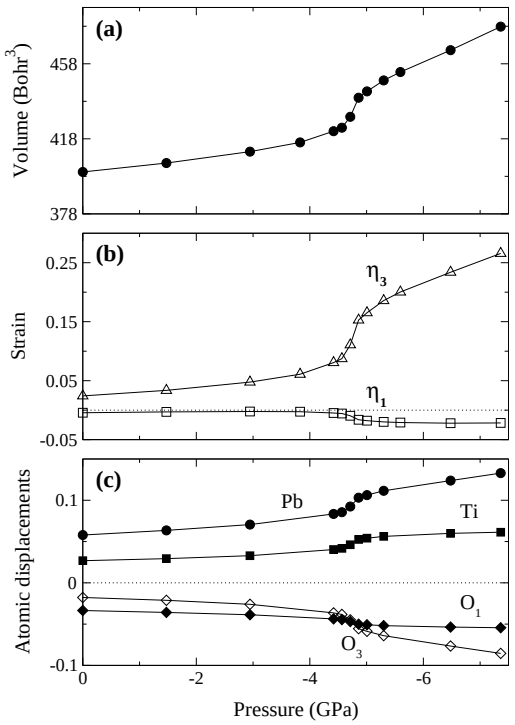

FIG. 1: Negative-pressure dependences of (a) volume (in Bohr^3); (b) tetragonal strain η_3 and η_1; (c) atomic displacements in the z direction (in c units) for tetragonal $PbTiO_3$.

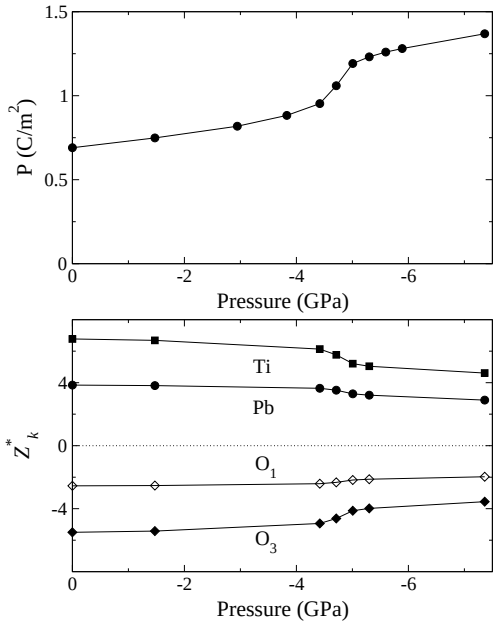

FIG. 2: Polarization (upper panel) and Born effective charges (Z^*_k) (bottom panel) for $PbTiO_3$ as a function of negative pressure.

III. RESULTS

A. Structural response

The observed crystal structure of ferroelectric $PbTiO_3$ has space group $P4mm$, with Pb in the (1a) Wyckoff position (0, 0, ξ_1), Ti in (1b)($\frac{1}{2}, \frac{1}{2}, \frac{1}{2} + \xi_2$), and O in (1b)($\frac{1}{2}, \frac{1}{2}, \xi_3$) and (2c) ($\frac{1}{2}, 0, \frac{1}{2} + \xi_4$) (0, $\frac{1}{2}, \frac{1}{2} + \xi_4$). The free structural parameters are the a lattice constant, the c/a ratio and the atomic displacements along $\hat{z}$, ξ_i (expressed in units of c). At zero pressure, our LDA calculation yields a T=0 equilibrium lattice constant of $a = 7.301$ a.u. and $c/a = 1.037$, which are $\sim -1\%$ and $\sim -3\%$ less than the experimental values of 7.373 a.u. and 1.065,[13] respectively. The fully-relaxed internal coordinates are $\xi_{Pb} = 0.0579$, $\xi_{Ti} = 0.0268$, $\xi_{O_1,O_2} = -0.0335$ and $\xi_{O_3} = -0.0177$, where O_1 and O_2 are the "in-plane" oxygens (2c) and O_3 is the apical (along $\hat{z}$ (1b)) oxygen of the Ti-centered oxygen octahedron. We use the convention that $\sum_k \xi_k = 0$. Throughout this work the reference state will be our theoretical minimum-energy ideal cubic structure ($a_0 = 7.331$ a.u.), in terms of which the strains are defined as $\eta_1 = (a - a_0)/a_0$ and $\eta_3 = (c - a_0)/a_0$.

We perform full, unconstrained optimization of the structural parameters of tetragonal $PbTiO_3$ as a function of external pressure ranging from 0 to -7 GPa. At a given pressure, the set of parameters that minimizes the total energy is determined. The negative-pressure dependence of the optimized structural parameters is shown in Fig. 1, where panels (a)-(c) display the unit-cell volume, strains (η_1 and η_3), and internal atomic displacements in the z direction, respectively. As can be seen from the figure, all of the structural parameters display an abrupt change around a crossover pressure $p_c \simeq -4.8$ GPa in a way that suggests proximity to a phase transition. The rapid enlargement of the unit-cell volume results from an abrupt increase of η_3, while it should be noted that the in-plane strain η_1 *decreases* slightly in the same pressure range. The net effect of the negative pressure is to stretch the unit cell strongly along $\hat{z}$ and slightly squeeze it in the plane. For example, just above the transition at $p = -5.3$ GPa, we find $\eta_1 = -0.02$ and $\eta_3 = 0.186$, and the resulting c/a is 1.21. Next, considering the relaxed atomic positions, the most remarkable feature is the change in character of the oxygen-displacement pattern. At pressures below p_c the apical oxygen is displaced less than the in-plane oxygens, whereas at pressures above p_c it is displaced more. At p_c both types of oxygens are displaced by nearly the same amount, which means that the oxygen cage forms a tetragonally strained octahedron.

For each of the optimized structures, we have also carried out spontaneous polarization calculations (upper panel of Fig. 2) as a function of negative pressure

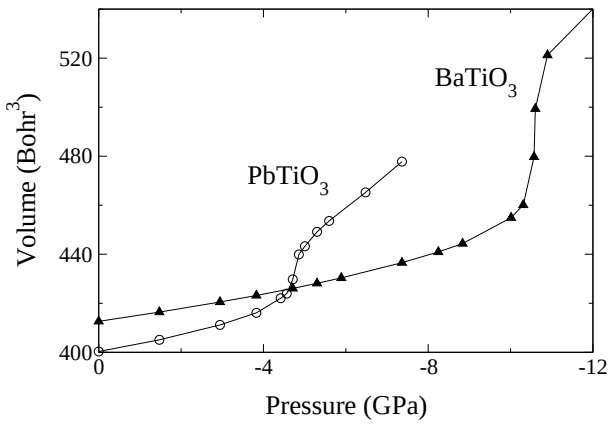

FIG. 3: Negative-pressure dependence of volume (in Bohr^3) for tetragonal $BaTiO_3$ and $PbTiO_3$.

using the Berry-phase theory of polarization.[14] It can be seen that the polarization shows the same kinky behavior at p_c. To get some insight into the polarization, we compute the Born effective charges (Z^*_k). The bottom panel of Fig. 2 shows $Z^*_{k,33}$ in the relaxed tetragonal structure at different pressures, as obtained by using density-functional perturbation theory. The results at zero pressure for k = Pb, Ti, O_1 and O_3 are 3.84, 6.77, −2.55, −5.50, similar to previously calculated values of 3.92, 6.71, −2.56, −5.51,[15] respectively. However, a direct comparison is not possible because the latter values were computed at the experimental tetragonal lattice constants. The most important features are the anomalously large effective charges of Ti and O_3 (oxygen along the bond) compared with their nominal charges (+4 and −2 respectively) and the anisotropy of the oxygen charge. These features persist throughout the negative-pressure range of interest, although all of the effective charges approach somewhat closer to the nominal values above p_c. Most notably, Z^*_{Ti} and $Z^*_{O_3}$ change by $\sim 25\%$ while passing through p_c, suggesting a weakening of the Ti–O bond, whereas Z^*_{Pb} and $Z^*_{O_1}$ decrease less noticeably. This follows the same trend observed in other perovskites,[16] where the Z^*'s decrease as the ions are displaced away from their high-symmetry cubic sites. The large changes in Z^*_{Ti} and $Z^*_{O_3}$ reflect the change of the Ti environment along the Ti–O chains; the shortened Ti–O_3 bonds remain almost constant in length while passing through p_c, while the elongated bonds lengthen abruptly there. Note that even though the Z^*'s decrease, the enhancement of the ionic displacements is so strong that the overall effect is a marked enhancement of the spontaneous polarization with negative pressure.

We have also investigated $BaTiO_3$ under negative pressure. In order to facilitate comparison with the results for $PbTiO_3$, we have imposed tetragonal symmetry, even though the ground state of $BaTiO_3$ is rhombohedral. Interestingly, we find the same anomalous effect as in $PbTiO_3$, but it occurs at much higher pressure in $BaTiO_3$. The computed optimized volume of $BaTiO_3$ in the tetragonal phase is plotted as a function of negative pressure in Figure 3, together with the corresponding results for $PbTiO_3$ for comparison. As seen, in $BaTiO_3$ the jump of the volume occurs at $p_c \simeq -10.6$ GPa, a pressure that is approximately twice as large as for $PbTiO_3$. Furthermore, the abrupt volume enhancement is even larger; in a pressure interval of width 1 GPa around p_c, the volume jump is $\sim 15\%$ in $BaTiO_3$, to be compared with $\sim 5\%$ in $PbTiO_3$.

B. Lattice instabilities

As a first step towards understanding the unexpected behavior of $PbTiO_3$ at negative pressures, we investigate the zone-center lattice instabilities in a structure having the lattice constants of the optimized tetragonal structure at the corresponding pressure, but without internal distortions (i.e., all atoms at centrosymmetric positions). For each structure, we compute the force-constant matrix at the Γ point using the frozen-phonon method.

The tetragonal ferroelectric phase of $PbTiO_3$ belongs to the C^1_{4v} ($P4mm$) space group. At the Γ point, the vibrational representation is spanned by two one-dimensional irreducible representations A_1 and B_1 and one two-dimensional representation E, of which there are 4, 1, and 5 copies, respectively, so that the force-constant matrix is block diagonal. As we are interested in the modes producing polarization along $\hat{z}$, we only have to diagonalize the 4×4 block of the A_1 subspace. The pure translational mode is discarded, and the eigenvalues (κ) of the three remaining A_1 modes are plotted versus pressure in Fig. 4. Negative values correspond to unstable modes. As expected, the ferroelectric soft mode is already unstable at zero pressure, and it becomes even more so as the crossover negative pressure region around $p_c = -4.8$ GPa is crossed because of the cell-volume enhancement that takes place there. However, we also find that a second mode becomes soft and that its frequency crosses through zero at a pressure that is close to the same p_c. At first sight, this concurrence might be taken as a hint of some connection between the second mode crossing and the anomalous "kinky" behaviors. However, as will be explained in Sec. IV, we think that if there is such a connection, it is more likely that the rapid expansion of the c lattice constant causes the second mode crossing, and not vice versa.

The corresponding eigenvectors are also very sensitive to pressure changes. Table I summarizes the eigenvalues κ and the eigenvectors of the original ferroelectric soft mode and the second soft mode at three different external pressures: zero, p_c, and a pressure higher than p_c. As can be seen, the original soft mode shows the displacement pattern that is typical of ferroelectric perovskites, with the cations moving in opposition to the oxygen octahedra. As the negative pressure increases,

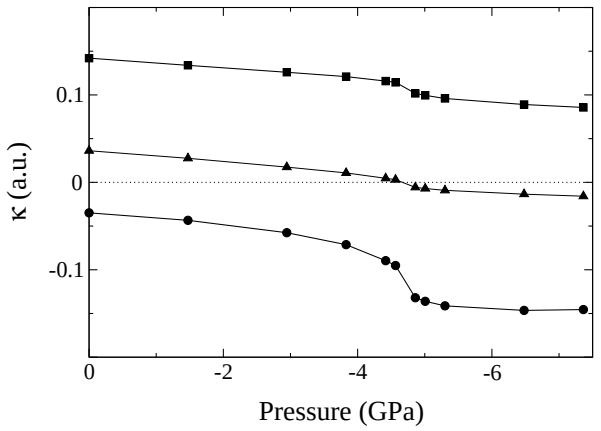

FIG. 4: Eigenvalues κ of the force-constant matrix in the centrosymmetric tetragonal structure with lattice constants of the optimized tetragonal structure at the specified pressure.

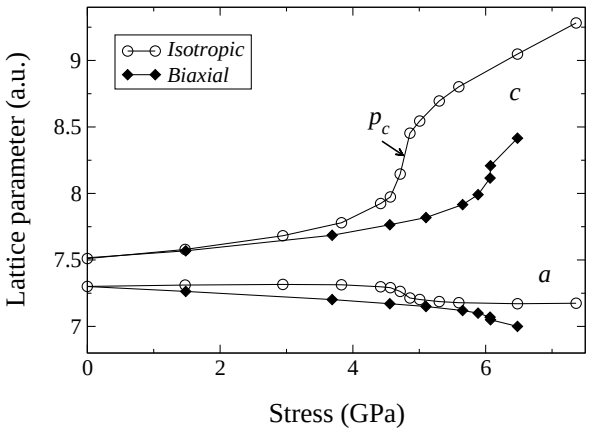

FIG. 5: Comparison of lattice parameters c and a, in a.u., as a function of absolute value of stress obtained for tetragonal $PbTiO_3$ by applying negative biaxial stress or positive isotropic stress (negative pressure).

the character of the mode evolves to one dominated by the long-short alternation of the bonds in the Ti-O bonds along $\hat{z}$. On the other hand, the pattern of the second soft mode consists mainly of the Pb–O_3 plane moving against the Ti–O_1 plane. At zero pressure the opposing cation displacements are dominant; negative pressure leads to an increase in the $O_{1,2}$ displacements and a decrease in the Ti displacement.

C. Applied biaxial stress

As mentioned in Sec. III A, the effect of negative isotropic pressure on the cell shape is to stretch the unit cell along $\hat{z}$ and slightly squeeze it in-plane. Here we consider what happens if instead we apply an in-plane stress only (σ_{xx}=σ_{yy} and σ_{zz}=0). This is effectively what happens in the case of epitaxial growth on a substrate of slightly different lattice constant.[17] In the calculation, we constrain the a lattice parameter and allow c and all the ionic positions in the [001] direction to relax while preserving the tetragonal space-group symmetry; the biaxial stress needed to support this structure is then computed directly within ABINIT.

TABLE I: Comparison of eigenvalues (κ) and eigenvectors of the original and second soft modes for different pressures. Eigenvectors (Pb, Ti, O_1=O_2, O_3) are normalized to unity.

	p (GPa)	κ (a.u.)	Eigenvector			
Original						
	0	−0.187	0.520	0.573	−0.388	−0.317
	−4.56	−0.308	0.217	0.752	−0.211	−0.546
	−6.48	−0.383	0.093	0.755	−0.108	−0.631
Second						
	0	0.190	0.713	−0.682	−0.076	0.121
	−4.56	0.056	0.824	−0.321	−0.317	0.130
	−6.48	−0.116	0.814	−0.128	−0.394	0.102

The results are shown in Fig. 5, where the lattice parameters are plotted for *expansive* (positive) isotropic stress (negative pressure) and for *compressive* (negative) in-plane stress. This is the appropriate comparison since both have the effect of enlarging the c lattice constant and thus potentially triggering the abrupt structural change. Indeed, we find that the biaxial stress *does* generate the same kind of anomalous c-axis behavior. The enlargement in c occurs at a somewhat larger magnitudes of the stress, and produces a somewhat more modest c-axis expansion, than for the isotropic-pressure case.

It should be emphasized, however, that the abrupt variation only appears when c and a are plotted vs. applied biaxial *stress*; simply plotting c vs. in-plane *strain* (i.e., vs. a) does not reveal anomalous behavior. Moreover, in order to obtain the same large c values that result near the kink in the negative-pressure case (indicated by p_c in the figure), we find that the in-plane lattice parameters would have to be compressed by $\sim -3.2\%$, which is much larger than the typical compression that can be attained by growth of $PbTiO_3$ on typical substrates such as $SrTiO_3$ ($\sim -1.4\%$)[18] or $NdGaO_3$ ($\sim -1\%$).[19] Thus, it does not appear that the predicted behavior can be observed in epitaxially strained films. Perhaps it may be possible to find some other way to generate a sufficiently large biaxial compressive stress so that this effect can be observed.

In any case, we think it is interesting that the application of compressive biaxial stress can generate the same kind of anomalous structural behavior as the application of negative isotropic pressure, at least for $PbTiO_3$. This result tends to support the speculation that some other kinds of variation (e.g., chemical substitution) might also be capable of driving a similar anomalous behavior.

D. Applied electric field

Another means of producing an effective tensile stress along $\hat{z}$ is the application of an electric field in the same direction. The induced polarization should couple strongly to the tetragonal strain. Therefore, we made a preliminary investigation of whether a strong applied electric field might be capable of inducing a similar anomalous enhancement of tetragonality. The structural parameters in applied electric fields can be estimated using an approximate scheme in which the *ab-initio* force on each atom (computed in zero electric field) is augmented by the product of the dynamical effective charge tensor for that atom and the applied electric field vector.[8,20] Based on our preliminary results, but more specifically on the results plotted in Fig. 8 of Ref. 8, it appears that η_3 and η_1 do *not* show any abrupt change up to 6×10^3 kV/cm. Thus, it seems unlikely that the application of an electric field can cause the same kind of anomalous behavior as the application of negative pressure. A more careful study would be desirable, checking whether the above approximations might be oversimplifying the treatment of some nonlinearities, but this is left for a future investigation.

IV. PHENOMENOLOGICAL MODEL DESCRIPTION

In order to explore the origins of the anomalous behavior that has emerged from our calculations in the vicinity of the crossover negative pressure p_c, we turn now to an attempt to model this behavior phenomenologically in terms of a reduced set of relevant degrees of freedom. We consider models similar to those that underlie the effective-Hamiltonian scheme,[6,21] in which the total energy is Taylor-expanded, in soft-mode and strain variables, about a reference cubic phase. The effect of the external hydrostatic pressure p is included by minimizing an enthalpy that includes a pV term in addition to the energy.

The first step in the construction of the model is to determine an appropriate set of degrees of freedom to be included. For practical reasons, this set should be as small as possible, and the definition of the degrees of freedom should not depend explicitly on pressure. Starting from a reference cubic structure, the fully relaxed structure at a given pressure can be separated into two parts: a homogeneous strain (leaving the atoms undistorted from their high-symmetry positions) and an "internal strain" (i.e., internal atomic displacements). To describe the first part, we make the simplest possible choice. As the unit-cell volume V increases monotonically with negative pressure, it specifies the strain state uniquely. This choice has the added convenience that it is V that directly couples to the pressure (it should be noted that the cell at given V will in general be tetragonal and its value of c and a are thus functions of V). Next, we need to find an appropriate basis able to capture the important internal strains at all relevant pressures. We first consider the entire set of zone-center modes of the cubic structure at zero pressure, and then attempt to determine which of these are most relevant for spanning the observed configurations in the pressure range of interest. Since the structure remains tetragonal, the three non-trivial A_1 modes form the starting point for this investigation. Let u, w and v denote the amplitudes of the softest, intermediate, and hardest mode of the force-constant matrix, with eigenvectors $|\varphi_u\rangle = |0.66, 0.39, -0.43, -0.43, -0.21\rangle$, $|\varphi_w\rangle = |0.60, -0.79, 0.10, 0.10, -0.01\rangle$ and $|\varphi_v\rangle = |0.06, 0.15, 0.33, 0.33, -0.87\rangle$, respectively. Then for each pressure, the optimized displacements shown in Fig. 1(c) are projected onto these three modes to obtain the amplitudes plotted in Fig. 6. As can be seen from the figure, the largest contribution at all pressures is clearly given by the soft mode u, while the other two appear less important. The contribution of the second mode is almost independent of pressure and can therefore be neglected. On the contrary, the highest-mode contribution is quite sensitive to pressure, increasing notably at p_c. The need to include at least one additional mode in the model subspace is clear from Figure 1(c), as a single mode cannot capture the change in character above p_c. The figure suggests that the highest-mode contribution v is next in importance after the soft mode u; the fact that including the v mode yields a qualitatively correct description of the distortions at all relevant pressures will be confirmed below.

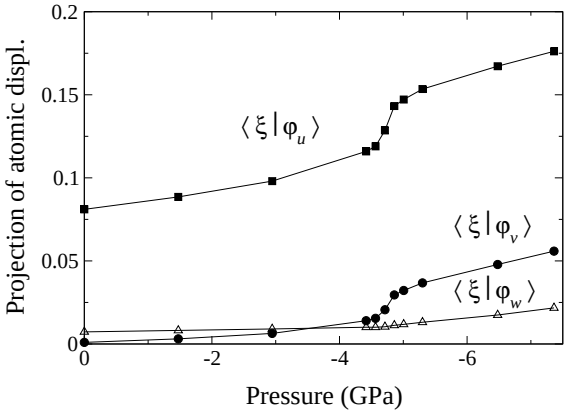

FIG. 6: Projection of the relaxed atomic displacements along $\hat{z}$ at the specified pressure ($\langle\xi|$) onto the three zone-center modes of the zero-pressure cubic structure ($|\varphi_u\rangle$, $|\varphi_v\rangle$ and $|\varphi_w\rangle$), given in units of c.

To develop the model, we consider the configuration subspace defined by three independent variables: the unit-cell volume V, the soft-mode amplitude u, and the hardest-mode amplitude v. At each volume V, we start by considering only the mode u (setting v=0), and

TABLE II: Parameters of the model total-energy expansion. All parameters are in atomic units.

V	A_0	4.4668	A_1	-0.0124	A_2	-5.69×10^{-5}
	A_3	2.37×10^{-7}	A_4	-2.17×10^{-10}		
u	C_{2u}	0.9264	C'_{2u}	-0.0042	C''_{2u}	4.65×10^{-6}
	C_{4u}	0.7095	C'_{4u}	-0.0030	C''_{4u}	3.18×10^{-6}
v	B_{1v}	0.6700	B'_{1v}	-1.64×10^{-3}		
	B_{2v}	-0.0851	B'_{2v}	5.16×10^{-4}		

Taylor-expand in u as

$$E(V,u) = E_0 + c_0(V) + c_{2u}(V)\,u^2 + c_{4u}(V)\,u^4\ , \quad (1)$$

where E_0 is the total energy at $V = V_0$ and $u = v = 0$, so that $c_0(V_0) = 0$, and terms of order u^6 and higher are dropped. The coefficients c_0, c_{2u} and c_{4u} are obtained by fitting to *ab-initio* total energies computed for configurations corresponding to various values of u, and the equilibrium value for $v = 0$ and fixed V is obtained by minimizing Eq. (1), leading to

$$u^2_{eq}(V) = -\frac{1}{2}\frac{c_{2u}(V)}{c_{4u}(V)} \quad (2)$$

and

$$E(V,u_{eq}(V)) = E_0 + c_0(V) - \frac{1}{4}\frac{c^2_{2u}(V)}{c_{4u}(V)}\ . \quad (3)$$

Then, starting at the configuration corresponding to $(u,v) = (u_{eq}(V),0)$, we compute *ab-initio* total energies for configurations corresponding to various values of v, holding V and $u = u_{eq}(V)$ fixed, and fit the result to quadratic order in v as

$$E(V,u_{eq}(V),v) = E(V,u_{eq}(V)) + b_{1v}(V)\,v + b_{2v}(V)\,v^2\ . \quad (4)$$

Minimizing the total energy with respect to v (at fixed V and $u = u_{eq}$), the equilibrium amplitude of this mode is obtained as

$$v_{eq}(V) = -\frac{1}{2}\frac{b_{1v}(V)}{b_{2v}(V)} \quad (5)$$

and the total energy is

$$E = E_0 + c_0(V) - \frac{1}{4}\frac{c^2_{2u}(V)}{c_{4u}(V)} - \frac{1}{4}\frac{b^2_{1v}(V)}{b_{2v}(V)}\ . \quad (6)$$

To facilitate the modeling of the dependence of these results on volume V, we fit the functions c_0, c_{2u}, c_{4u}, b_{1v}, and b_{2v} as polynomials in V:

$$c_0(V) = A_0 + A_1V + A_2V^2 + A_3V^3 + A_4V^4\ , \quad (7)$$

$$c_{2u}(V) = C_{2u} + C'_{2u}V + C''_{2u}V^2\ , \quad (8)$$

$$c_{4u}(V) = C_{4u} + C'_{4u}V + C''_{4u}V^2\ , \quad (9)$$

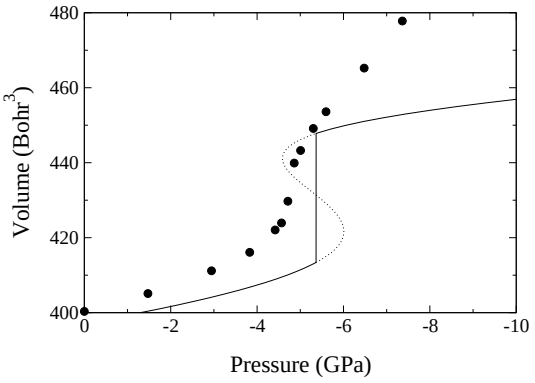

FIG. 7: Pressure computed at different volumes by using the phenomenological model (full line) compared with the first-principles results (circles).

$$b_{1v}(V) = B_{1v} + B'_{1v}V\ , \quad (10)$$

$$b_{2v}(V) = B_{2v} + B'_{2v}V\ . \quad (11)$$

The expansion parameters were determined by fitting to the results of total-energy calculations in the interval of volumes from 400 to 480 a.u.^{3}, near $V_0 = 393.99$ a.u.^{3}. The resulting parameters of the model are reported in Table II.

We then explored the behavior of this model by determining the equilibrium structural parameters as a function of pressure p, minimizing the enthalpy $H = E + pV$. The result is shown by the solid line in Fig. 7. We find that there is a pressure interval from about -4.6 to -6 GPa in which two local minima compete, with a first-order isostructural transition between minima at $p_c \simeq -5.4$ GPa. The locations of the secondary minimum and the saddle point are indicated by the dotted line in Fig. 7, obtained by evaluating the thermodynamic relation $p = -\partial E(V)/\partial V$ as a function of V.

Comparing the behavior of the model with the first-principles results, shown as solid circles in Fig. 7, we see that the model correctly reproduces the existence of an abrupt variation of structural parameters with negative pressure. In fact, the model even goes too far, exhibiting a true first-order transition where there is none in the first-principles results. The model also slightly overestimates, by about 10-15%, the magnitude of the negative pressure at which the abrupt change occurs, and underestimates the pressure dependence of the volume at the highest negative pressures.

Even with these minor discrepancies, the model is very useful in generating a clearer picture of the observed behavior. In particular, the fact that a first-order transition occurs in the model supports the idea that the anomalous enhancement of tetragonality in the first-principles calculations results from proximity to a phase transition. To make this idea more precise, we consider small variations

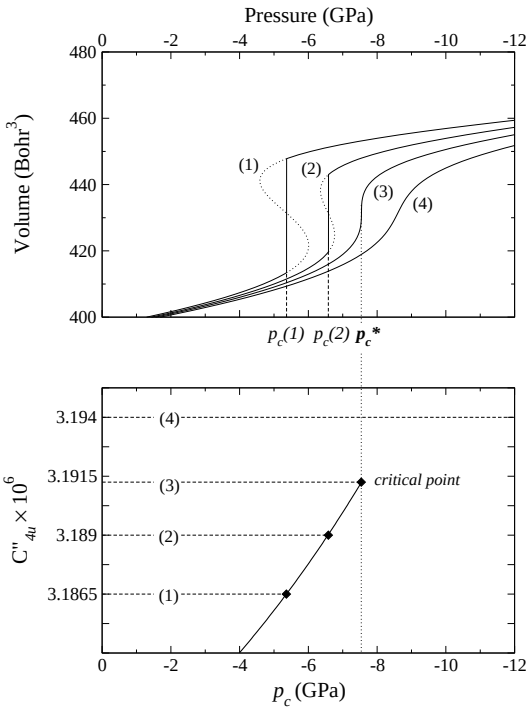

FIG. 8: Calculated $P-V$ phase diagram for different C''_{4u} parameters (upper panel). The original model is marked as case (1). C''_{4u} parameter–critical pressure (p_c) diagram (bottom panel). For values bigger than C''_{4u} at the critical point there is no phase transition.

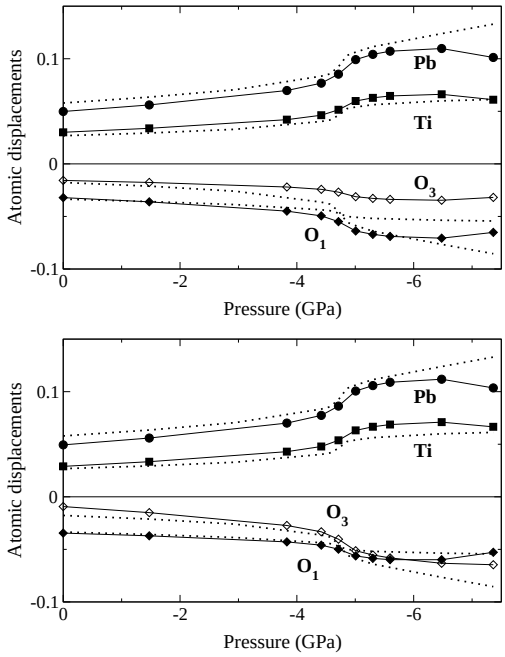

FIG. 9: Configurational space described by u_{eq} (upper panel) and by u_{eq} and v_{eq} (bottom panel) compared with the minimum-energy structures (dotted lines).

of one of the model parameters, C''_{4u}, keeping all other parameters fixed, and study the transition behavior as a function of pressure. The upper panel of Fig. 8 shows the P–V diagram for four different values of C''_{4u}, starting from the original model marked as case (1) and increasing C''_{4u} incrementally to case (4). As can be seen, for the smaller values of C''_{4u} there is a first-order phase transition from a low-c/a to a high-c/a phase at a transition pressure p_c (cases (1) and (2)). The volume discontinuity decreases with increasing C''_{4u} and vanishes at a triple point (case (3)). In other words, a critical value of the C''_{4u} parameter exists above which there is no distinction between two phases (see, e.g., case (4)). The relation between C''_{4u} and the transition pressure is presented in the bottom panel of Figure 8; the phase boundary defined in this way terminates at the triple point identified by pressure p_c^*.

Thus, Fig. 8 demonstrates that with increasing negative pressure, $PbTiO_3$ passes very close to a triple point. In fact, it passes so close that the errors introduced by the truncations and simplifications of our model, described earlier in this section, are sufficient to cause the model system to exhibit a true first-order phase transition. Indeed, to shift the model system into the transition-free region of parameter space, it suffices to change C''_{4u} by only $\sim 0.15\%$. A more accurate model containing additional fitting parameters (e.g., an independent treatment of lattice constants c and a, inclusion of mode w, and/or a more careful treatment of cross terms between modes u and v) would presumably be sufficient to reproduce the observed "kinky" behavior without the spurious first-order transition.

We now turn to an examination of the role of the additional mode v in the anomalous negative-pressure behavior of $PbTiO_3$. The effects of holding v=0 can be easily obtained by minimizing the enthalpy $E+pV$ with E from Eq. (3). The V vs. p curve still exhibits the anomalous negative-pressure behavior, although the transition region is considerably shifted (to around -12 GPa) and there is no first-order transition in this case (similar to the first-principles result). Thus, inclusion of the additional mode v is not absolutely necessary to produce the anomalous negative-pressure behavior. On the other hand, neglecting this mode leads to a substantial quantitative error in the transition pressure. Moreover, as we have already seen in Fig. 1(c) and Fig. 6, the inclusion of the mode v is needed to correctly capture the variation of the atomic displacements with pressure. This point is emphasized in Fig. 9. In the upper panel, the ratios of the displacements are fixed with an overall amplitude proportional to u (shown with symbols), so that it is impossible to reproduce the crossing in the oxygen displacement pattern around p_c. In the lower panel, the inclusion of the v mode yields a qualitative improvement,

with a crossing close to p_c. The discrepancy between the model and the first-principles results (shown with dotted lines) grows much more noticeable above p_c. This most likely reflects the contribution of the neglected modes and couplings to the strong pressure dependence above p_c, which is underestimated by the model.

Finally, we analyze the relation between the modes of the centrosymmetric tetragonal structure (dependent on pressure) and the modes u, v and w, used in the construction of our model. In our discussion of Fig. 4 in Sec. III B, we noted that the tetragonal mode of intermediate hardness crosses from positive to negative κ (i.e., from stable to unstable behavior) at a pressure very close to that at which the anomalous structural response occurs. Projecting the pressure-dependent tetragonal modes on the cubic modes, we find that the tetragonal soft mode is mainly described by the mode u at all pressures, with a significant contribution of the mode w above p_c, whereas the tetragonal mode of intermediate hardness is mainly described at lower pressures by the mode w, and then above p_c by the mode v. Since the kinky behavior occurs even when both cubic-structure modes v and w are frozen to zero amplitude, we think that it is unlikely that the zero crossing of the second tetragonal-structure mode has a *causal* role in the anomalous structural behavior. Instead, it seems more likely that it simply *results* from the abrupt expansion of the c-axis lattice parameter.

Thus, we believe that the model developed in this section, based on an expansion of the total energy with respect to the volume and two zone-center mode amplitudes, is a reasonable compromise between simplicity and accuracy. It gives a good qualitative and even semi-quantitative description of the abrupt variation of the structural parameters near p_c. The fact that it predicts a true first-order transition at p_c, instead of a smooth but "kinky" cross-over, should be taken more as a sign of the proximity of the real system to a phase transition than as a failure of the model. We are hopeful that this model will be useful for investigating and describing similar behavior in other perovskite systems.

V. DISCUSSION AND SUMMARY

We have shown that the application of negative pressure induces a large enhancement of tetragonal strain in tetragonal $PbTiO_3$. Specifically, in a window of pressure centered around a particular value p_c, c/a abruptly increases, and all structural parameters exhibit a corresponding "jump" that suggests proximity to a phase transition.

To describe this unexpected behavior in $PbTiO_3$, we have generated a phenomenological model from our *ab initio* results, based on an expansion of the total energy with respect to a carefully selected subset of the structural degrees of freedom. This has led to the identification of a phase boundary, analogous to the liquid-gas phase boundary, in the model parameter space. With the parameters obtained from fitting to first-principles total energies of $PbTiO_3$, the model predicts not just a "kinky" behavior, but a true first-order transition at a critical pressure p_c close to the pressure at which the anomaly occurs in the first-principles calculations. We found that a tiny variation of one parameter is sufficient to drive the model through a triple point and bring it to a transition-free portion of parameter space where the "kinky" behavior is qualitatively well-reproduced. It might become possible to realize such variations of effective model parameters by some combination of "external fields" such as chemical substitution, temperature, epitaxial stress, or homogeneous electric field. If so, one might develop experimental techniques for turning the transition off or on, tuning the associated transition properties, and perhaps even exploring the region of the triple point itself.

Finally, we speculate that this "anomalous" behavior of the structural parameters of tetragonal $PbTiO_3$ could be a more general feature in perovskite oxides. For example, we have found that the same anomalous behavior is also present in $BaTiO_3$ with imposed tetragonal symmetry (though at much higher negative pressure), so that a similar phase boundary could be explored in this portion of perovskite parameter space. The possibility of analogous transitions in other ABO_3 perovskites is under investigation. This could present tantalizing opportunities for designing perovskite-based materials with large and controllable strain variations.

Acknowledgments

We would like to thank Na Sai for providing the initial suggestion for the direction of this work. This work was supported by the Center for Piezoelectrics by Design (CPD) under ONR Grant N00014-01-1-0365. Computational facilities for the work were also provided by the CPD. We thank Morrel Cohen for useful discussions.

[1] S.-E. Park, T. R. Shrout, J. Appl. Phys. **82** 1804 (1997). S.-E. Park, W. Hackenberger, Curr. Opin. Solid State Mater Sci. **6**, 11 (2002).
[2] B. Noheda, D. E. Cox , G. Shirane, S.-E. Park, L. E. Cross, Z. Zhong, Phys. Rev. Lett. **86** 3891 (2001).
[3] B. Noheda, D. E. Cox , G. Shirane, J. Gao, Z. G. Ye, Phys. Rev. B **66** 054104 (2002).
[4] R. E. Cohen, Nature **258**, 136 (1992).
[5] A. García and D. Vanderbilt, Phys. Rev. B **54**, 3817 (1996).
[6] U. V. Waghmare and K. M. Rabe, Phys. Rev. B **55**, 6161 (1997).
[7] G. Sághi-Szabó, R. E. Cohen and H. Krakauer, Phys. Rev. Lett. **80**, 4321 (1998).

[8] Na Sai, Karin M. Rabe and David Vanderbilt, Phys. Rev. B **66**, 104 108 (2002).
[9] ABINIT is a common project of the Université Catholique de Louvain, Corning Incorporated, and other contributors (http://www.abinit.org). X. Gonze, J.-M. Beuken, R. Caracas, F. Detraux, M. Fuchs, G.-M. Rignanese, L. Sindic, M. Verstraete, G. Zerah, F. Jollet, M. Torrent, A. Roy, M. Mikami, Ph. Ghosez, J.-Y. Raty, D.C. Allan, Comput. Mater. Sci. **25**, 478-492 (2002).
[10] J. P. Perdew and Y. Wang, Phys. Rev. B **45**, 13 244 (1992).
[11] D. Ceperley, Phys. Rev. B **18**, 3126 (1978); D. M. Ceperley and B. J. Alder Phys. Rev. Lett. **45**, 566 (1980).
[12] M. Teter, Phys. Rev. B **48**, 5031 (1993).
[13] G. Shirane, R. Pepinsky and B. C. Frozer, Acta Crystallogr. **9**, 131, (1956).
[14] R. D. King-Smith and D. Vanderbilt, Phys. Rev. B **47**, 1651 (1993).
[15] W. Zhong, R. D. King-Smith and D. Vanderbilt, Phys. Rev. Lett. **72**, 3618 (1994).
[16] Ph. Ghosez, J. P. Michenaud, X. Gonze, Phys. Rev. B **58**, 6224 (1998).
[17] N. A. Pertsev, A. G. Zembilgotov, A. K. Tagantsev, Phys. Rev. Lett. **80**, 1988 (1998).
[18] Y.-F. Chen, L. Sun, T. Yu, J.-Y. Chen, N.-B. Ming, D.-S. Ding, L.-W. Wang, Appl. Phys. Lett. **67**, 3503 (1995).
[19] L. Sun, Y.-F. Chen, L. He, Ch.-Z. Ge, D.-S. Ding, T. Yu, M.-S. Zhang, N.-B. Ming, Phys. Rev. B **55**, 12 218 (1997).
[20] H. Fu and L. Bellaiche, private communication.
[21] W. Zhong, D. Vanderbilt and K. M. Rabe, Phys. Rev. Lett. **73**, 1861 (1994).